OncoTargets and Therapy

Dovepress
open access to scientific and medical research

Open Access Full Text Article

ORIGINAL RESEARCH

PSAT1 Regulated Oxidation-Reduction Balance Affects the Growth and Prognosis of Epithelial Ovarian Cancer

This article was published in the following Dove Press journal:
OncoTargets and Therapy

Yiqun Zhang[1–3,*]
Jiajia Li[1–3,*]
Xuhui Dong[1–3]
Dan Meng[4]
Xiuling Zhi[4]
Lei Yuan[1–3]
Liangqing Yao[1–3]

[1]Department of Gynecology, Obstetrics and Gynecology Hospital of Fudan University, Shanghai, People's Republic of China; [2]Shanghai Medical College, Fudan University, Shanghai, People's Republic of China; [3]Shanghai Key Laboratory of Female Reproductive Endocrine-Related Diseases, Fudan University, Shanghai, People's Republic of China; [4]Department of Physiology and Pathophysiology, School of Basic Medical Sciences, Shanghai, People's Republic of China

*These authors contributed equally to this work

Introduction: A growing number of studies have found that the serine-glycine biosynthesis pathway is highly activated for biosynthesis in cancer progression and metastasis. Phosphoserine aminotransferase 1 (PSAT1) catalyzes the second step of the serine-glycine biosynthesis pathway; the effects and mechanism of PSAT1 in epithelial ovarian cancer (EOC) remains unclear.

Materials and Methods: The expression of PSAT1 in clinical EOC samples and normal ovarian tissues was conducted by RT-PCR, Western blot, and immunohistochemical staining. Survival analysis of PSAT1 in ovarian cancer was performed by using the public database. Following the downregulation of PSAT1, the cell growth, cell apoptosis, and cell cycle in ovarian cancer cells were respectively examined by the soft agar colony formation assay and flow cytometry analysis. Then the glutathione (GSH) levels, the GSH/GSSG ratio, the NADPH/NADP ratio, and the cellular reactive oxygen species (ROS) levels were tested to analyze the oxidation-reduction balance in PSAT1-depleted ovarian cancer cells.

Results: PSAT1 is markedly over-expressed in clinical EOC samples (n = 90) compared to that in normal ovarian tissues (n = 10), and the expression of PSAT1 is correlated with histological subtype, FIGO stage, histological grade, lymph node metastasis, distant metastasis and the presence of ascites. Public database analysis shows that higher PSAT1 indicates poor survival in EOC patients. Downregulation of PSAT1 in EOC cells inhibits growth, induces apoptosis and cell cycle arrest in vitro. EOC cells with high PSAT1 levels have increased a higher GSH (reduced glutathione)/GSSG (oxidized glutathione) ratio and lower reactive oxygen species (ROS) content. The cancer-killing effects of PSAT1 knockdown are reversed by exogenous glutathione. PSAT1 participates in cancer growth by regulating oxidation-reduction balance.

Conclusion: Therefore, these results highlight the potential of PSAT1 inhibitors or metabolic substrate deprivation as therapeutic strategies for treating patients with EOC, especially those with advanced stages of cancer.

Keywords: phosphoserine aminotransferase 1, oxidative stress, serine-glycine biosynthesis pathway, epithelial ovarian cancer

Introduction

The mortality rate of ovarian cancer is in first place in gynecologic tumors. The five-year survival rate of ovarian cancer is only from 30% to about 50%. Ovarian cancer patients are not presented with typical clinical symptoms and serum tumor markers at the early stage, making it difficult for early diagnosis. Sometimes the primary focus is not large, but ovarian cancer can be very aggressive and often

Correspondence: Lei Yuan; Liangqing Yao
Department of Gynecology, Obstetrics and Gynecology Hospital of Fudan University, Shanghai 200011, People's Republic of China
Tel +86-18964075180
Email ylronda@163.com; yaoliangqing@163.com

submit your manuscript | www.dovepress.com
DovePress
http://doi.org/10.2147/OTT.S250066

metastasize in pelvic and peritoneal cavity with poor prognosis.[1] Thus, exploring the occurrence and progression mechanisms of EOC has become a research hotspot in molecular oncology.

Phosphoserine aminotransferase 1 (PSAT1), is a member of the class-V pyridoxal-phosphate-dependent aminotransferase family. During the second step in the serine-glycine biosynthesis pathway, PSAT1 catalyzes a glutamate-linked transamination reaction to convert 3-phosphohydroxypyruvate into L-phosphoserine.[2] Previous studies found that PSAT1 plays important regulatory roles in tumorigenesis and malignant progression.[3] Inhibition of PSAT1 promotes DNA damage and apoptosis.[4,5] PSAT1 increases resistance in melanoma, pancreatic, and non-small cell lung cancer cells.[6] High PSAT1 expression is found in triple-negative breast cancer and is closely associated with aggressive frequently metastasizes and clinical prognosis.[7] PSAT1 promotes cisplatin resistance and angiogenesis via activating GSK3β/β-catenin signaling pathway.[8] PSAT1 also affects mouse embryonic stem cell differentiation via α-ketoglutarate, a metabolite regulated by Oct4/Sox2/Nanog.[9] However, the detailed functions and molecular mechanism of PSAT1 in EOC remains unknown.

The imbalance of redox state is one of the important characteristics of malignant tumors. Highly reactive oxygen species (ROS) has been detected in cancer tissue and has multiple functions.[10] At the same time, ROS can activate DNA repair pathways to counteract DNA damage and genomic instability. Cancer promoting effects of the serine-glycine biosynthesis pathway involve the production of folic acid, methionine, and vitamin B6, which contributes to reduced glutathione (GSH) synthesis.[11] GSH was significantly involved in oxidative stress. GSH levels associate with chemosensitivity and programmed cell death of tumor cells.[12,13] However, the content and the effect of GSH in EOC have not been fully researched.

In our work, a significant over-expression of PSAT1 is found in EOC and correlates with poor prognosis. Down-regulation of PSAT1 inhibits the clonogenicity, cell cycle and promotes apoptosis. PSAT1 expression increases the proportion of GSH and reduced nicotinamide adenine dinucleotide phosphate (NADPH) in EOC cells, increasing oxidative stress tolerance. The antitumor effects of PSAT1 knockdown were altered by reduced glutathione administered in the medium. Thus, PSAT1 contributes to oxidation-reduction balance, resulting in the malignant development of EOC. Our findings suggest that PSAT1 may serve as a potential diagnostic biomarker and therapeutic target for ovarian cancer.

Materials and Methods

Tissue Datasets

Differentially expressed genes between normal ovarian tissues and EOC samples of gene data (GSE52460, GSE27651) were analyzed using a WEB-based gene set analysis tool (https://www.gcbi.com.cn, Genminix Informatics Ltd., Co, Gminix, Shanghai, China). Screening criteria for differential genes: Q value < 0.05, $P < 0.05$, Fold change > 2. Heat maps were generated based on the differential genes between normal ovarian tissues and EOC samples. The genes whose expression was up-regulated > 10 times in ovarian cancer tissues in both chips were screened as candidates for the study. The GO term enrichment and pathway analysis of differential gene expression were carried out using the gene set analysis tool. The PSAT1 expression level of normal and cancer tissues were retrieved from the Cancer Genome Atlas (TCGA; 594 samples in GSE220892 of ovarian cancer), Okayama Lung (246 samples in GSE223062 of lung cancer), and Hong Colorectal (82 samples in GSE223062 of colorectal cancer) databases and analyzed using Oncomine (https://www.oncomine.org). Survival analysis of mRNA gene chip (GSE26193, GSE30161, GSE51373, GSE9891) was conducted using the Kaplan–Meier Plotter (http://www.kmplot.com) with auto-selection of best cutoff values.

Human EOC Data

The research using ovarian cancer samples and normal ovarian tissues was approved by the ethical committee of the Obstetrics and Gynecology Hospital of Fudan University (approval ID, No. 2017–39). Our study was conducted in accordance with the Declaration of Helsinki. All clinical samples were obtained with patient written informed consent. Ninety EOC specimens and ten normal ovary specimens were collected from the Obstetrics and Gynecology Hospital of Fudan University from November 2013 to November 2018. All cases meet the following criteria: histopathologic diagnosis, random selection, complete follow-up, no other history of cancer, and no preoperative radiation or chemotherapy. Tissue within 2cm from the lesion was identified as adjacent ovarian tissues. The staging system for ovarian cancer is the International Federation of Gynecology and Obstetrics (FIGO) staging system. Normal ovarian tissues were from the removed ovary in the operation of benign gynecological diseases.

Cell Culture

Human ovarian cancer cell lines ES2, HEY, HO8910, OVCAR-3, SKOV3, SKOV3-IP, and the normal ovarian epithelial cell line HOSEpiC were obtained from Cell Bank of Shanghai Institute (Cell Bank of Shanghai Institute of Cell Biology at the Chinese Academy of Sciences, Shanghai, China). The cells were analyzed using short tandem repeat sequence and tested for mycoplasma and cell viability. All cells were cultured to exponential phase in RPMI 1640 complete medium (Thermo Fisher Scientific, Waltham, MA, USA) with 10% fetal bovine serum in a 5% CO_2 incubator at 37°C. The additive reduced glutathione was purchased from Sigma-Aldrich.

Recombinant Plasmids and Transfection

All short hairpin RNA (shRNA) plasmids for inhibiting PSAT1 were designed by GenePharma Company (GenePharma, Shanghai, China). The detailed target sequences are listed in Supplementary Table 1. The target sequence of shRNA329 was finally adopted as the experimental group for the further experiments: 5′-GCTGTTCCAGACAACTATA AG-3′. The sequence of non-targeting control shRNA (Con shRNA) was used as a control group: 5′-GTTCTCCGA ACGTGTCACGT-3′. SKOV3 and HO8910 cells were transfected with PSAT1 shRNA or Con shRNA using Lipofectamine 3000 according to the manufacturer's protocol (Thermo Fisher Scientific, Waltham, MA, USA).

Construction of Lentiviruses and Infection

hU6-MCS-CMV-puromycin lentiviral vectors (GV112) were purchased from GeneChem Company (GenePharma, Shanghai, China). Lentiviral vectors carrying a PSAT1 shRNA plasmid were constructed to inhibit PSAT1 expression in SKOV3 and HO8910 cells. Puromycin was added to select stable clones.

RNA Isolation and Quantitative Real-Time PCR

The total RNA was extracted from cell lines and ovarian tissues using RNAsimple Total RNA kit (Tiangen Biotech, Beijing, China). Reverse transcript cDNA was synthesized using PrimeScriptTMRT Master Mix (Takara, Shiga, Japan). Quantitative real-time PCR (RT-PCR) was conducted using SYBR Premix EX Taq II (Takara, Shiga, Japan) on a 7500 RT-PCR system (Applied Biosystems, Foster City, CA). Glyceraldehyde 3-phosphate dehydrogenase was used as the control for normalization. Primers were designed and synthesized Sangon Company (Sangon Biotech, Shanghai, China). Detailed primer sequences of PSAT1 are listed: Forward, TGTGGTGACAGGAGCTTGGT; Reverse: GG TTGAGGTTCCAGGTGCTT.

Western Blot

Cells and ovarian tissues were lysed in radioimmunoprecipitation assay buffer with protease inhibitor cocktail and PhosSTOP (Roche, Basel, Switzerland). Protein extraction was analyzed using a bicinchoninic acid quantitation kit (Beyotime, Beijing, China). After 4–12% sodium dodecyl sulfate polyacrylamide gel electrophoresis, proteins were transferred to a polyvinylidene difluoride membrane with primary antibodies, followed by horseradish peroxidase–linked secondary antibodies (Abcam, Hongkong, Chian) and enhanced chemiluminescence reagents (Millipore Corp., Billerica, MA, USA). All antibodies used are listed in Supplementary Table 2.

Proliferation Assays

To measure cell proliferation, 3.5×10^4 SKOV3 and 7×10^4 HO8910 cells infected by recombinant lentiviral vectors were plated onto 12-well plates, then cultured in complete medium supplemented with or without an additional 5 mM reduced glutathione for 120 hours. Cells were collected for direct cell counting using an automatic cell counter.

Soft Agar Colony Formation Test

Cells mixed with soft agar were plated on 35-mm dishes and cultured for 14 days. Cell colonies were fixed with 4% paraformaldehyde for 30 min and stained with 2% crystal violet solution for 1 hour. The number of colonies was counted randomly from five different areas at low magnification.

Cell Apoptosis Assay

A fluorescein isothiocyanate annexin V apoptosis detection kit (BD Biosciences, San Diego, CA, USA) was used to detect cell apoptosis. Cells were resuspended in 1X binding buffer (1×10^6 cells/mL) and incubated with fluorescein isothiocyanate annexin V and propidium iodide for 20 min at 25°C in the dark. Within 1 hour, the number of apoptotic cells was counted using flow cytometry.

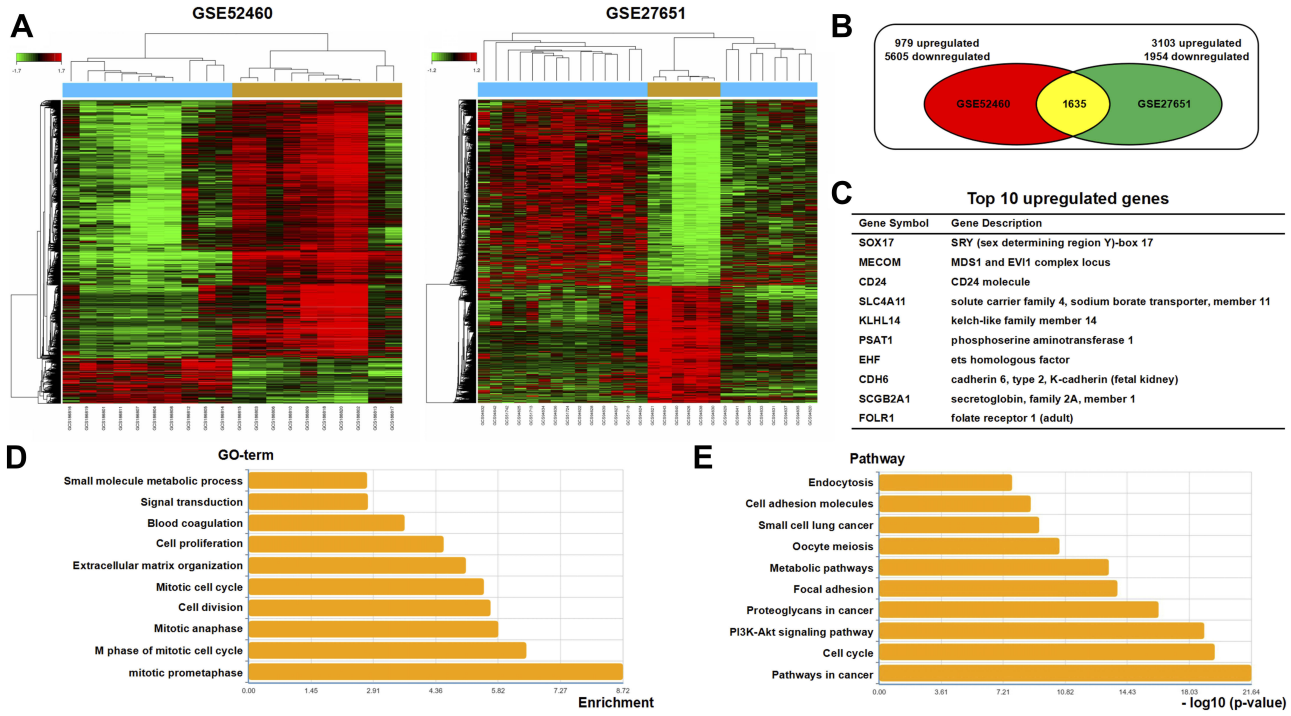

Figure 1 Overexpression of PSAT1 in EOC tissues. Two microdissected profiling datasets (GSE52460, GSE27651) were used for transcriptomic analysis. Both datasets included serous ovarian carcinoma and normal ovarian tissues. (**A**) Clustering of differentially expressed genes in EOC datasets. Fold Change > 2, $P < 0.05$. (**B**) Venn diagram of analysis results using the microdissected profiling datasets of EOC tissues. (**C**) Top 10 upregulated differentially expressed genes most associated with EOC tumorigenesis. (**D**) TOP 10 enriched GO terms in differentially expressed genes. (**E**) TOP 10 enriched pathways in differentially expressed genes.

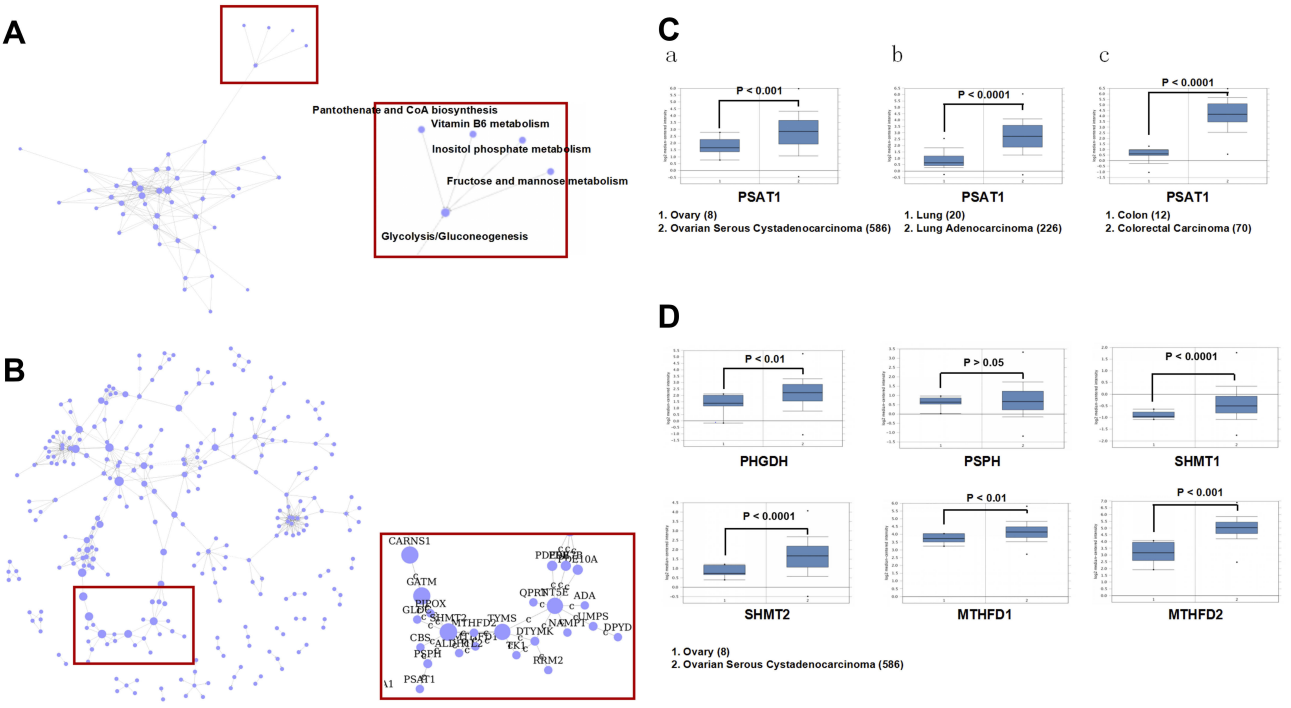

Figure 2 Identification of PSAT1 as a novel biomarker in EOC tissues. (**A**) The pathway relation network indicated that vitamin B6 metabolism was associated with EOC tumorigenesis. (**B**) Gene signal network indicated that key enzymes in the serine-glycine synthesis pathway were associated with EOC tumorigenesis. (**C**) PSAT1 mRNA levels (Oncomine) in (a) normal ovary versus ovarian serous cystadenocarcinoma (TCGA data), (b) normal lung versus lung adenocarcinoma (Okayama Lung data), (c) normal colon versus colorectal carcinoma (Hong Colorectal data). (**D**) The mRNA levels of PHGDH, PSPH, SHMT1, SHMT2, MTHFD1, and MTHFD2 (Oncomine) were analyzed in normal ovary versus ovarian serous cystadenocarcinoma.

Cell Cycle Assay

Ovarian cancer cells were suspended in 5 mL cold 70–80% ethanol and stored at 4°C away from light overnight. Cells were washed with phosphate-buffered saline and stained with 0.5 mL propidium iodide/RNase buffer for 15 min at 25°C in the dark. Cells in different phases (G0/G1, S, G2/M) were counted by flow cytometry.

Immunohistochemical Staining

Histological sections from tissues were obtained from ninety EOC patients and ten patients with benign gynecological diseases. The slides were incubated with anti-PSAT1 (Proteintech, Chicago, LA, USA). Five fields of view (40 X) in each slide were randomly selected, and then calculated the average IHC staining score of each slide. The results of the PSAT1 IHC staining were determined using the following criteria: PSAT1 IHC score = staining intensity × staining quantity. Staining intensity was divided into four levels: negative (0 point), weak (1 point), moderate (2 points), and strong (3 points). Staining quantity was divided into four levels: negative (0 points); positive area < 25% (1 point); 25% ≤ positive area < 50% (2 points); and positive area ≥ 50% (3 points).

GSH/GSSG Detection

The levels of GSH, GSSG and GSH/GSSG ratio in cells and tissues were detected via a GSH/GSSG-Glo™ Assay (Beyotime, Shanghai, China) following the manufacturer's instructions and measured using a microplate reader.

NADPH/NADP Detection

The NADPH/NADP ratio in cells was detected via an NADPH/NADP Detection Kit (Beyotime, Shanghai, China) following the manufacturer's instructions and measured using a microplate reader.

ROS Detection

The ROS content in cells and tissues was detected via a ROS-GloTM H2O2 assay kit (Beyotime, Shanghai, China). Relative luminescence units were measured using a microplate reader or a FACS Calibur flow cytometer.

Statistical Analysis

All data were analyzed by GraphPad Prism 5.0 and presented as mean ± standard errors of the mean. The values between the two groups were compared with Student's *t*-test. One-way ANOVA with post hoc tests was used to

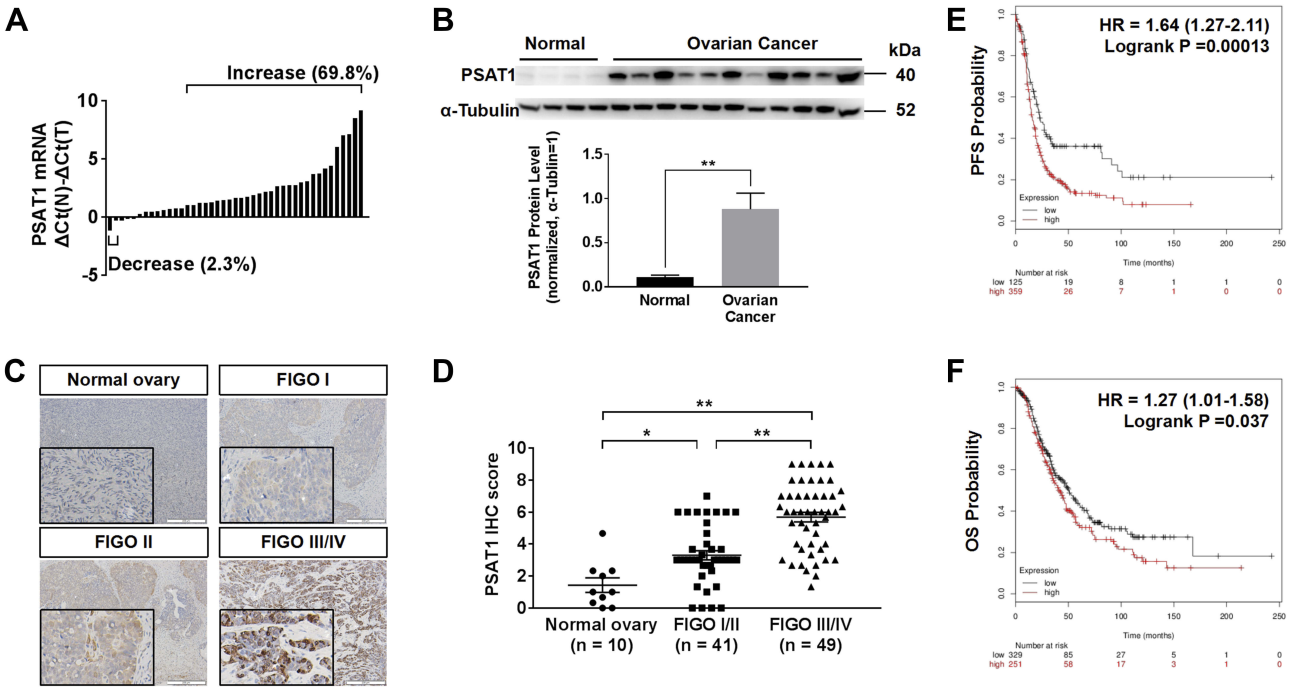

Figure 3 Up-regulation of PSAT1 in EOC correlated with poor prognosis. (**A**) Relative PSAT1 mRNA levels in 43 EOC tissues and 6 normal ovarian tissues. Bar value ≤ −1 indicates that PSAT1 was reduced; ≥ 1 indicates that PSAT1 was elevated in tumors. (**B**) Western blot analysis of PSAT1 in 11 EOC tissues and 4 normal ovarian tissues. α-Tubulin was used as the loading control. *T*-test, $^{**}P < 0.01$. Error bars in panels are defined as SEM. (**C**) Representative immunohistochemistry (IHC) images of PSAT1 expression in ovarian cancer tissues of different stages. Scale bar, 200 μm. (**D**) Scatter plots of IHC scores from FIGO stage I/II to III/IV of EOC specimens. ANOVA with post hoc tests, $^{**}P < 0.01$, $^{*}P < 0.05$. (**E, F**) Kaplan–Meier analysis of progression-free survival (PFS) and overall survival (OS) of EOC patients categorized by PSAT1 expression determined by mRNA gene chip.

analyze values among multiple groups. Chi-squared analysis was used to determine the association between PSAT1 level and the clinicopathological characteristics of EOC patients. Survival curves were created using Kaplan–Meier Plotter with the Log rank test. A P value of less than 0.05 indicated a significant difference.

Results

PSAT1 Is Upregulated in EOC and Associates with Tumorigenesis

To investigate the regulatory molecules that drive tumor growth in EOC, we analyzed overlapping genes with 979 genes in GSE52460 and 3103 genes in GSE27651 that were significantly highly expressed in EOC tissues compared to those in normal ovarian tissues (Figure 1A and B). We identified the top ten differentially expressed genes, enriched GO terms and pathways in EOC (Figure 1C–E). PSAT1 was significantly high expressed, and relatively metabolic pathways were active. The Pathway relation network showed that EOC had strong vitamin B6 metabolism (Figure 2A). The activity of PSAT1 is regulated by pyridoxine phosphate. The latter is the active form of vitamin B6. Gene signal network showed that key enzymes in the serine-glycine synthesis pathway were associated with EOC tumorigenesis (Figure 2B). The higher expression of PSAT1 in EOC was also confirmed in gene chips datasets of ovarian, lung, and colorectal cancer (Figure 2C). Meanwhile, PHGDH, SHMT1, SHMT2 in serine glycine synthesis pathway, and MTHFD1, MTHFD2 in downstream folic acid synthesis pathway were also abnormally higher in EOC (Figure 2D). Thus, PSAT1 in metabolic pathways was selected as a candidate target in EOC therapy.

The Abnormal Increase of PSAT1 Correlates with Poor Prognosis

According to RT-PCR analysis of RNA extraction from EOC and normal ovarian tissues, PSAT1 at the RNA level was higher in 30 of 43 (69.8%) EOC tissues than in normal ovarian tissues; only 1 (2.3%) EOC tissue showed lower PSAT1 expression (Figure 3A). Immunoblot analysis of protein lysates from eleven EOC tissues and four normal ovarian tissues further indicated that PSAT1 expression was higher in EOC tissues than in normal ovarian tissues (Figure 3B). The PSAT1 expression level was closely associated with tumor progression of EOC from FIGO stage I/II (early-stage) to III/IV (advanced stage) (Figure 3C and D). Table 1 shows that PSAT1 expression was related to histological subtype, FIGO stage, histological grade, lymph node metastasis, distant metastasis, and the presence of ascites. Survival analysis

Table 1 Association of PSAT1 Expression with Clinicopathological Features in EOC Patients

Variable	Low PSAT1 Expression (n=45)	High PSAT1 Expression (n=45)	*P*
	n (%)	n (%)	
Age (years)			
<50	12(26.7)	13(28.9)	0.814
≥50	33(73.3)	32(71.1)	
Histological subtype			
Other	9(20.0)	2(4.4)	0.024
Serous	36(80.0)	43(95.6)	
FIGO stage			
I–II	31(68.9)	10(22.2)	0.000
III–IV	14(31.1)	35(77.8)	
Histological grade			
Low	10(22.2)	2(4.4)	0.013
High	35(77.8)	43(95.6)	
Tumor size (cm3)			
<1000	39(86.7)	38(84.4)	0.764
≥1000	6(13.3)	7(15.6)	
Number of tumors			
<2	24(53.3)	28(62.2)	0.393
≥2	21(46.7)	17(37.8)	
Residual tumor diameter (cm)			
<1	43(95.6)	41(91.1)	0.398
≥1	2(4.4)	4(8.9)	
Lymph node metastasis			
Absent	38(84.4)	24(53.3)	0.001
Present	7(15.6)	21(46.7)	
Distant metastasis			
Absent	43(95.6)	37(82.2)	0.044
Present	2(4.4)	8(17.8)	
CA125 level (U/mL)			
<600	29(64.4)	23(51.1)	0.200
≥600	16(35.6)	22(48.9)	
Ascites			
Absent	23(51.1)	12(26.7)	0.017
Present	22(48.9)	33(73.3)	

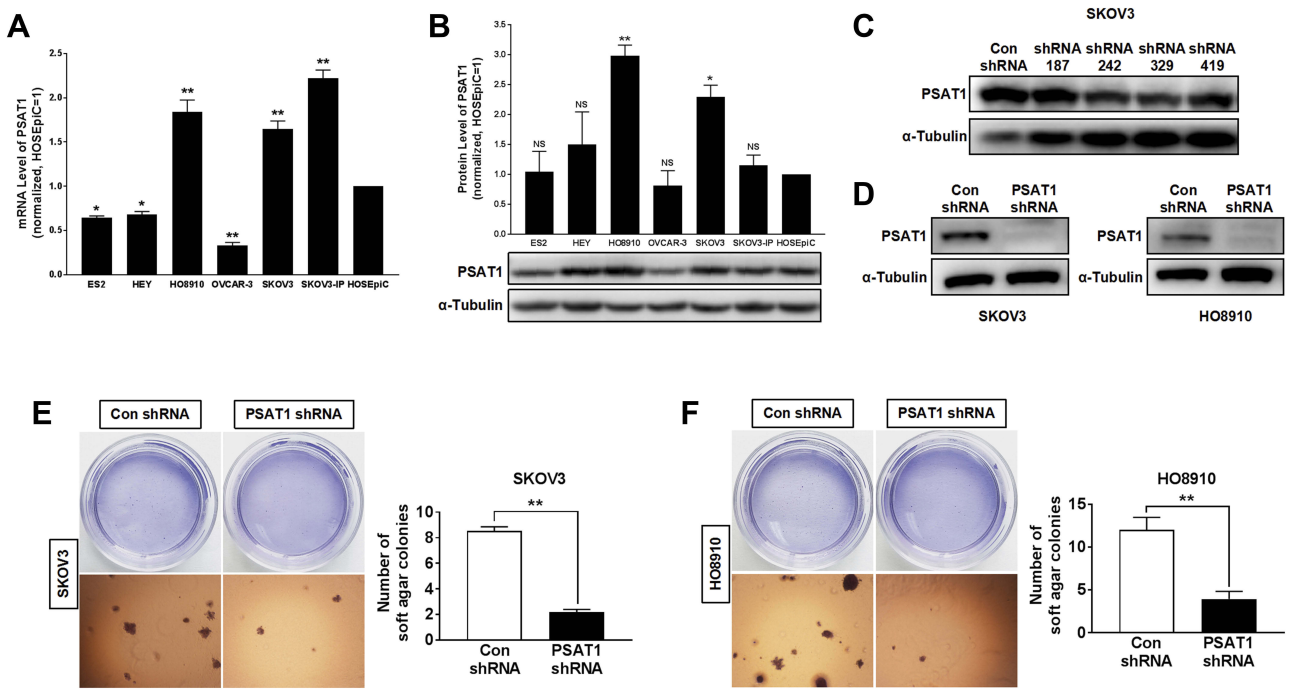

Figure 4 Knockdown of PSAT1 inhibited tumorigenicity of EOC cells in vitro. (**A**) PSAT1 mRNA levels in ES2, HEY, HO8910, OVCAR-3, SKOV3, SKOV3-IP, and normal ovarian epithelial cell line HOSEpiC (n = 3). $^{**}P < 0.01$, $^{*}P < 0.05$ vs HOSEpiC, ANOVA with post hoc tests. (**B**) Western blot analysis of PSAT1 and α-Tubulin in ovarian cancer cell lines (lower); the normalization expression of PSAT1 (upper) (n = 3). α-Tubulin was used as a control. $^{**}P < 0.01$, $^{*}P < 0.05$ vs. HOSEpiC, ANOVA with post hoc tests. (**C**) Western blot analysis of PSAT1 and α-Tubulin for SKOV3 cells transfected with nonspecific shRNA (Con shRNA) or PSAT1-specific shRNA (shRNA 187, shRNA 242, shRNA 329, and shRNA 419). (**D**) Western blot analysis of PSAT1 and α-Tubulin for SKOV3 and HO8910 cells transfected with lentivirus-mediated shRNA 329 interference vectors (PSAT1 shRNA). (**E**) Histograms represent the quantification of colony formation of SKOV3 with or without stable PSAT1 knockdown in soft agar under low magnification. Scale bar = 500 μm (n = 3). *T*-test, $^{**}P < 0.01$. (**F**) Histograms represent the quantification of colony formation of SKOV3 with or without stable PSAT1 knockdown in soft agar under low magnification. Scale bar = 500 μm (n = 3). *T*-test, $^{**}P < 0.01$. All error bars in panels are defined as SEM.

Abbreviation: NS, not significant.

using Kaplan–Meier Plotter revealed that patients with high *PSAT1* expression showed significantly worse progression-free survival (PFS; n=484, Log rank test P = 0.00013, Figure 3E) and overall survival (OS; n=580, Log rank test P = 0.037, Figure 3F) than those with low *PSAT1* expression. Taken together, these results indicate that PSAT1 expression correlates with malignancy, resulting in a poor prognosis for patients with EOC.

PSAT1 Is Essential for Tumor Growth in vitro

In evaluating PSAT1 expression in EOC cell lines, we identified SKOV3 and HO8910 cells as those with the highest PSAT1 expression (Figure 4A and B). SKOV3 and HO8910 cells were then used for subsequent experiments. We designed four shRNAs (shRNA187, shRNA242, shRNA329, and shRNA419) targeting PSAT1. Their efficiencies of PSAT1 knockdown in SKOV3 were quantified by immunoblotting analysis (Figure 4C). The shRNA329 was selected to construct a lentiviral vector. After transfection by the lentiviral vector, puromycin was added to select stably transfected cell lines. We confirmed the stable knockdown of PSAT1 in SKOV3 and HO8910 cells before conducting further experiments (Figure 4D). PSAT1 knockdown suppressed clonogenicity (Figure 4E and F). Furthermore, PSAT1 knockdown increased the rate of early and total apoptosis (Figure 5A), and its inhibitory effect on proliferation was related to blocking the cell cycle at the G0/G1 phase (Figure 5B). Immunoblotting further confirmed that PSAT1 knockdown attenuated the expression of Cyclin D1 and CDK4. In addition, PSAT1 knockdown also promoted the expression of Bax and cleaved Caspase-3 (Figure 5C and D). These findings suggested that PSAT1 is critical for cell cycle progress and viability.

PSAT1 Promotes Malignant Development by Inhibiting Oxidative Stress

Inhibition of PSAT1 reduced the GSH/GSSG and NADPH/NADP ratios, indicating that PSAT1 regulates the production of reducing equivalents (Figure 6A and B). PSAT1 knockdown inhibited the serine-glycine biosynthesis pathway toward GSH and NADPH production. NADPH and

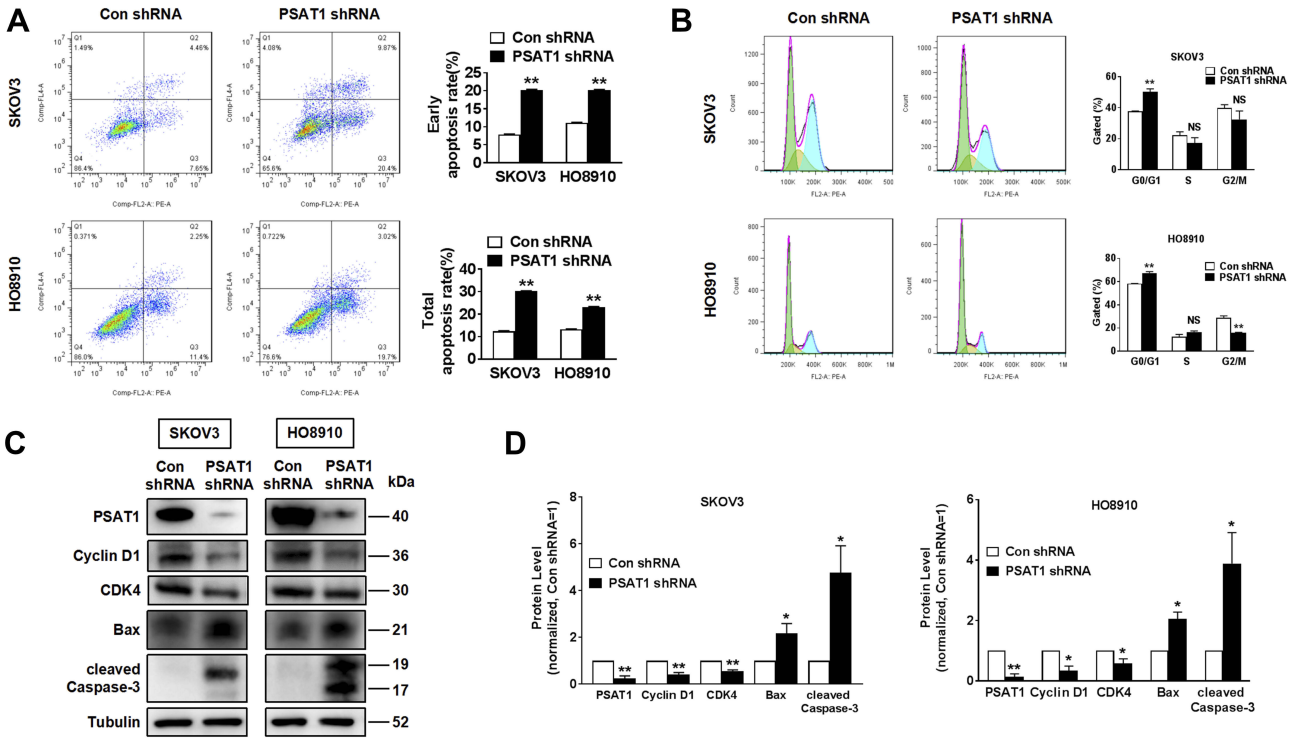

Figure 5 Knockdown of PSAT1 promoted apoptosis and inhibited cell cycle of EOC cells in vitro. (**A**) Flow cytometry analysis of apoptosis of SKOV3 and HO8910 cells without or with stable PSAT1 knockdown (n = 3). *T*-test, $^{**}P < 0.01$. (**B**) Flow cytometry analysis of the cell cycle stages of SKOV3 and HO8910 cells without or with stable PSAT1 knockdown (n = 3). *T*-test, $^{**}P < 0.01$. (**C, D**) Western blot and histograms of PSAT1, Cyclin D1, Bax, cleaved Caspase-3, and α-Tubulin for SKOV3 and HO8910 cells with or without PSAT1 knockdown. (n = 3). *T*-test, $^{**}P < 0.01$, $^{*}P < 0.05$. All error bars in panels are defined as SEM.

GSH play an important physiological role as the delivery of hydrogen, which is involved in oxidative stress. The GSH/GSSG and NADPH/NADP ratios reflect the oxidative stress levels. Thus, we detected intracellular ROS in EOC cells following PSAT1 knockdown. PSAT1 knockdown significantly increased intracellular ROS levels (Figure 6C). We further found that exogenous GSH (5 mM) restored cell proliferation following inhibition of PSAT1 (Figure 6D). Consistent with these results, the addition of exogenous GSH (5 mM) had a reverse effect of PSAT1 knockdown on Cyclin D1 and cleaved Caspase-3 (Figure 6E). Given that PSAT1 might regulate the redox status in EOC, the PSAT1 and ROS levels of ovarian cancer tissue were evaluated compared with adjacent and normal ovarian tissues (n=3) (Figure 6F). Consistent with our previous findings, PSAT1 expression was significantly higher in ovarian cancer than normal ovarian tissues (n=3) (Figure 6G). EOC tissues show a higher ROS level compared with normal ovarian tissues. High ROS level suggested high oxidative stress status in EOC tissues. Increased levels of GSH and GSH/GSSG ratio were observed in ovarian cancer tissue compared with adjacent and normal ovarian tissues (n=3) (Figure 6H and I). It seems that PSAT1 activation protected cells from oxidative damage via GSH production.

Discussion

Cancer is dependent on metabolic reprogramming.[14] Previous work on molecule-targeted tumor therapy has shown that completely inhibiting oncogenes is not as effective as expected and is usually accompanied by compensatory glucose or glutamine metabolism.[15] These studies have underscored the importance of glucose and glutamine metabolism for cancer therapy.[16] The serine-glycine biosynthesis pathway is a crucial component of the glucose and glutamine metabolic network. Several studies have shown that high PSAT1 expression is implicated in malignant metastasis, chemosensitivity, and poor outcomes.[6,7,17] Inhibiting PSAT1 has been found to enhance the sensitivity of non-small cell lung cancer cells in the absence of glutamine.[18] Dai et al found that silencing PSAT1 reduced angiogenesis and cisplatin resistance via GSK3β/β-catenin pathway.[8] Although many malignant tumors have shown active PSAT1 in the serine-glycine biosynthesis pathway,[4,19,20] the role of it in ovarian cancer is yet unclear at present.

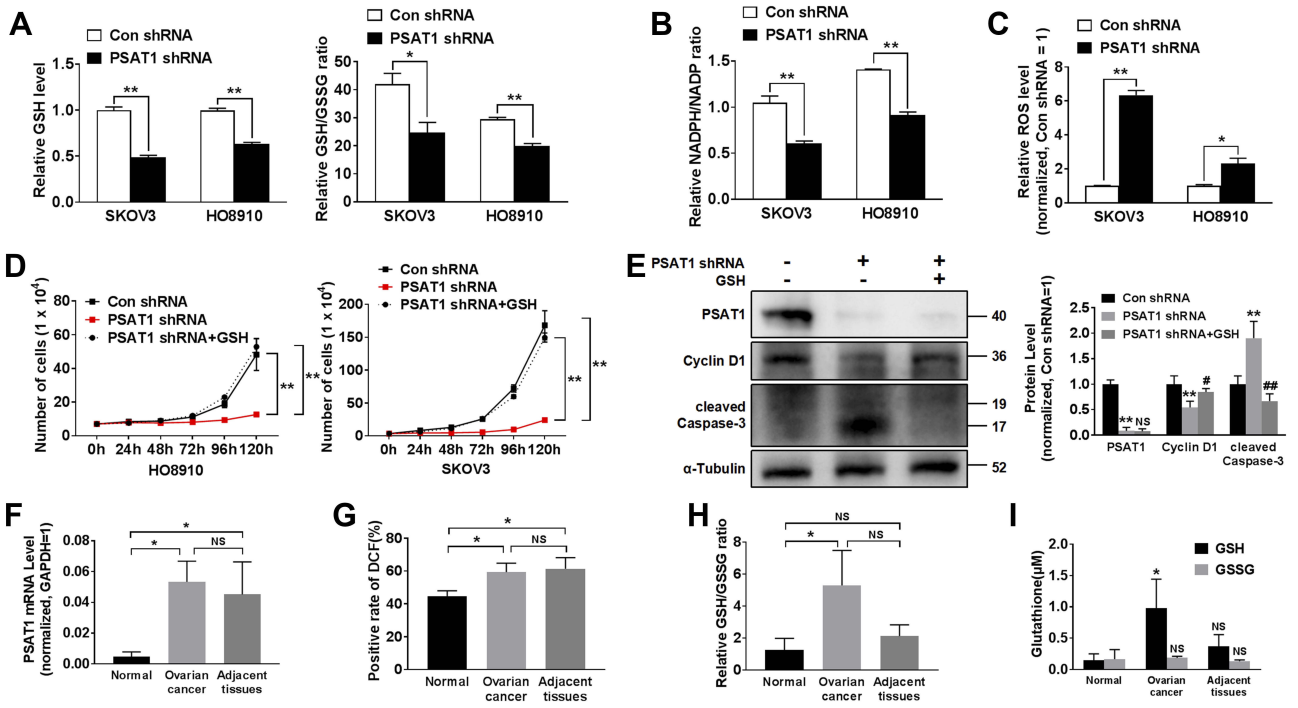

Figure 6 PSAT1 promotes the growth of EOC by regulating redox balance. (**A**) Glutathione (GSH) levels and the GSH/GSSG ratio were calculated in SKOV3 and HO8910 cells without or with stable PSAT1 knockdown (n = 3). *T*-test, $^{**}P < 0.01$, $^{*}P < 0.5$. (**B**) The NADPH/NADP ratio was calculated in SKOV3 and HO8910 cells without or with stable PSAT1 knockdown (n = 3). *T*-test, $^{**}P < 0.01$. (**C**) Cellular reactive oxygen species (ROS) levels were determined in SKOV3 and HO8910 cells without or with stable PSAT1 knockdown (n = 3). *T*-test, $^{**}P < 0.01$, $^{*}P < 0.05$. (**D**) Proliferation assays of PSAT1-knockdown SKOV3 and HO8910 cells in medium with or without supplemental GSH (n = 3). *T*-test, $^{**}P < 0.05$ vs Con shRNA. (**E**) Western blot and histograms of PSAT1, Cyclin D1, cleaved Caspase-3, and α-Tubulin for PSAT1-knockdown SKOV3 cells with or without supplemental GSH. (n = 3). $^{**}P <$ 0.01 vs Con shRNA; $^{\#}P < 0.05$ vs PSAT1 shRNA, $^{\#\#}P < 0.01$ vs PSAT1 shRNA. ANOVA with post hoc test. (**F**) PSAT1 mRNA levels in normal ovary, ovarian cancer, and adjacent tissue (n=3). ANOVA with post hoc test. $^{*}P < 0.5$. (**G**) Rate of intracellular ROS activation was monitored by DCF in normal ovary, ovarian cancer, and adjacent tissue (n=3). ANOVA with post hoc test. $^{*}P < 0.5$. (**H**) The GSH/GSSG ratio was calculated in normal ovary, ovarian cancer, and adjacent tissue (n=3). ANOVA with post hoc test. $^{*}P < 0.5$. (**I**) GSH and GSSG levels in normal ovary, ovarian cancer, and adjacent tissue (n=3). ANOVA with post hoc test. $^{*}P < 0.5$ vs normal. All error bars in panels are defined as SEM.

Abbreviation: NS, not significant.

Data demonstrates that PSAT1 showed the potential to become a prognostic marker.[21] The result is consistent with our findings. We found that PSAT1 was upregulated in EOC tissues, and its expression was correlated with some malignant clinicopathological characteristics (Table 1) and poor prognosis (Figure 3). Our studies further indicate the role and mechanism of PSAT1 in the malignant development and oxidative stress of EOC. While there are multiple antagonists of PHGDH, a key enzyme in the serine-glycine biosynthesis pathway.[22] The investigation of PSAT1 antagonists remains limited. The antimalarial agent artemether was used as an inhibitor of PSAT1 to treat *Acanthamoeba* infections.[23] A study investigated the structure and strong inhibitory response of halide on PSAT1 from *Trichomonas vaginalis*.[24] Moreover, PSAT1 can catalyze the reversible transformation of 3-phosphohydroxypyruvate to L-phosphoserine with glutamate as a substrate. Because the arginine and histidine residues (Arg42, Arg328, His41, and His327) form a tight binding site for the phosphate group of L-phosphoserine, L-phosphoserine analogs that bind to these residues may be effective agents.[25] It is necessary to strengthen research on developing PSAT1 antagonists.

Research suggests that abnormal tumor metabolism led to high oxidative stress status, while cancer cells maintained the ability to proliferate against the oxidative stress.[26,27] The detailed role of PSAT1 against oxidative stress in EOC has not been described. We now show that inhibition of PSAT1 have decreased GSH and NADPH flux, produced oxidative stress, and inhibited tumor growth (Figure 6). High activated oxygen concentration is the signal that starts the apoptosis. The effect of PSAT1 knockdown could be restored by exogenous GSH, which was consistent with previous work that indicated a positive correlation between GSH uptake and the proliferation of prostate and breast cancer cells.[28] Assay of oxidative stress from surgical samples of EOC patients confirmed that high PSAT1 expression could improve GSH synthesis. In our work, GSH is essential for the growth and survival of EOC cells, contrary to previous reports of antioxidants improving human health and achieving longevity.[29] Antioxidant

nutrients have been an essential part of health care products with the lack of safety and efficacy data. There was a suggestion that antioxidants and vitamins increased the risk of recurrence for breast cancer.[30] PSAT1 belongs to the class-V pyridoxal-phosphate-dependent aminotransferase family. Pyridoxal-5′-phosphate is an intermediate of vitamin B6 metabolism. When vitamin B6 is absorbed by the body, it can be converted into pyridoxal-5′-phosphate in the liver. Thus, our data presented that uses of antioxidants and vitamin B6 should be with caution.

The limitation of this study is that we did not perform GSH treatment in the mouse model. Moreover, a large dose of ROS may induce mitochondrial dysfunction, destroy the activities of mitochondrial enzymes. Thus, associations between PSAT1 and mitochondrial function need to be studied. There's still a lot of work to do to understand the relationship between GSH application and ovarian cancer prognosis.

Our data shows that PSAT1 expression stimulates GSH synthesis and promotes ovarian cancer progression in high oxidative stress status. Future research work should be focused on mitochondrial changes caused by PSAT1 activation and GSH accumulation. In summary, our study emphasizes the role of PSAT1 and provides the basis for potential treatments targeting PSAT1 in ovarian cancer.

Acknowledgments

This study was supported by the Chinese National Natural Sciences Foundation (grant number 81571401, 81601235).

Author Contributions

LQ.Y. and L.Y. designed and supervised the progression of the study. YQ.Z. carried out most experiments, analyzed the data, and drafted the manuscript. JJ.L. carried out some experiments and helped revised the manuscript. XH.D., D. M., and XL.Z. assisted with some of the experiments. All authors have reviewed the manuscript. All authors contributed to data analysis, drafting or revising the article, gave final approval of the version to be published, and agree to be accountable for all aspects of the work.

Disclosure

The authors declare no potential conflicts of interest.

References

1. Pignata S, Cannella L, Leopardo D, Pisano C, Bruni GS, Facchini G. Chemotherapy in epithelial ovarian cancer. *Cancer Lett*. 2011;303(2):73–83. doi:10.1016/j.canlet.2011.01.026
2. Basurko MJ, Marche M, Darriet M, Cassaigne A. Phosphoserine aminotransferase, the second step-catalyzing enzyme for serine biosynthesis. *IUBMB Life*. 1999;48(5):525–529. doi:10.1080/713803557
3. Yang Y, Wu J, Cai J, et al. PSAT1 regulates cyclin D1 degradation and sustains proliferation of non-small cell lung cancer cells. *Int J Cancer*. 2015;136(4):E39–E50. doi:10.1002/ijc.29150
4. Sen N, Cross AM, Lorenzi PL, et al. EWS-FLI1 reprograms the metabolism of ewing sarcoma cells via positive regulation of glutamine import and serine-glycine biosynthesis. *Mol Carcinog*. 2018;57(10):1342–1357. doi:10.1002/mc.22849
5. Amelio I, Cutruzzola F, Antonov A, Agostini M, Melino G. Serine and glycine metabolism in cancer. *Trends Biochem Sci*. 2014;39(4):191–198. doi:10.1016/j.tibs.2014.02.004
6. Ross KC, Andrews AJ, Marion CD, Yen TJ, Bhattacharjee V. Identification of the serine biosynthesis pathway as a critical component of BRAF inhibitor resistance of melanoma, pancreatic, and non-small cell lung cancer cells. *Mol Cancer Ther*. 2017;16(8):1596–1609. doi:10.1158/1535-7163.MCT-16-0798
7. Metcalf S, Dougherty S, Kruer T, et al. Selective loss of phosphoserine aminotransferase 1 (PSAT1) suppresses migration, invasion, and experimental metastasis in triple negative breast cancer. *Clin Exp Metastasis*. 2019.
8. Dai J, Wei R, Zhang P, Kong B. Overexpression of microRNA-195-5p reduces cisplatin resistance and angiogenesis in ovarian cancer by inhibiting the PSAT1-dependent GSK3beta/beta-catenin signaling pathway. *J Transl Med*. 2019;17(1):190. doi:10.1186/s12967-019-1932-1
9. Hwang IY, Kwak S, Lee S, et al. Psat1-dependent fluctuations in alpha-ketoglutarate affect the timing of ESC differentiation. *Cell Metab*. 2016;24(3):494–501. doi:10.1016/j.cmet.2016.06.014
10. Moloney JN, Cotter TG. ROS signalling in the biology of cancer. *Semin Cell Dev Biol*. 2018;80:50–64. doi:10.1016/j.semcdb.2017.05.023
11. Smith CL, Bolton A, Nguyen G. Genomic and epigenomic instability, fragile sites, schizophrenia and autism. *Curr Genomics*. 2010;11(6):447–469. doi:10.2174/138920210793176001
12. Butturini E, Carcereri de Prati A, Boriero D, Mariotto S. Natural sesquiterpene lactones enhance chemosensitivity of tumor cells through redox regulation of STAT3 signaling. *Oxid Med Cell Longev*. 2019;2019:4568964. doi:10.1155/2019/4568964
13. Lv H, Zhen C, Liu J, Yang P, Hu L, Shang P. Unraveling the potential role of glutathione in multiple forms of cell death in cancer therapy. *Oxid Med Cell Longev*. 2019;2019:3150145. doi:10.1155/2019/3150145
14. Li AM, Ducker GS, Li Y, et al. Metabolic profiling reveals a dependency of human metastatic breast cancer on mitochondrial serine and one-carbon unit metabolism. *Mol Cancer Res*. 2020;18(4):599–611. doi:10.1158/1541-7786.MCR-19-0606
15. Tanaka K, Sasayama T, Irino Y, et al. Compensatory glutamine metabolism promotes glioblastoma resistance to mTOR inhibitor treatment. *J Clin Invest*. 2015;125(4):1591–1602. doi:10.1172/JCI78239
16. Marengo B, Garbarino O, Speciale A, Monteleone L, Traverso N, Domenicotti C. MYC expression and metabolic redox changes in cancer cells: a synergy able to induce chemoresistance. *Oxid Med Cell Longev*. 2019;2019:7346492. doi:10.1155/2019/7346492
17. Qian C, Xia Y, Ren Y, Yin Y, Deng A. Identification and validation of PSAT1 as a potential prognostic factor for predicting clinical outcomes in patients with colorectal carcinoma. *Oncol Lett*. 2017;14(6):8014–8020. doi:10.3892/ol.2017.7211
18. Jin HO, Hong SE, Kim JY, et al. Knock-down of PSAT1 enhances sensitivity of NSCLC cells to glutamine-limiting conditions. *Anticancer Res*. 2019;39(12):6723–6730. doi:10.21873/anticanres.13887
19. Selvarajah B, Azuelos I, Plate M, et al. mTORC1 amplifies the ATF4-dependent de novo serine-glycine pathway to supply glycine during TGF-β1–induced collagen biosynthesis. *Sci Signal*. 2019;12(582):eaav3048. doi:10.1126/scisignal.aav3048

20. Li K, Wu JL, Qin B, et al. ILF3 is a substrate of SPOP for regulating serine biosynthesis in colorectal cancer. *Cell Res*. 2020;30(2):163–78.
21. Zheng MJ, Li X, Hu YX, et al. Identification of molecular marker associated with ovarian cancer prognosis using bioinformatics analysis and experiments. *J Cell Physiol*. 2019;234(7):11023–11036. doi:10.1002/jcp.27926
22. Ravez S, Spillier Q, Marteau R, Feron O, Frederick R. Challenges and opportunities in the development of serine synthetic pathway inhibitors for cancer therapy. *J Med Chem*. 2017;60(4):1227–1237. doi:10.1021/acs.jmedchem.6b01167
23. Deng YH, Ran W, Man SG, et al. Artemether exhibits amoebicidal activity against *Acanthamoeba castellanii* through inhibition of the serine biosynthesis pathway. *Antimicrob Agents CH*. 2015;59 (8):4680–4688. doi:10.1128/AAC.04758-14
24. Singh RK, Mazumder M, Sharma B, Gourinath S. Structural investigation and inhibitory response of halide on phosphoserine aminotransferase from. *BBA-Gen Subjects*. 2016;1860(7):1508–1518. doi:10.1016/j.bbagen.2016.04.013
25. Battula P, Dubnovitsky AP, Papageorgiou AC. Structural basis of L-phosphoserine binding to *Bacillus alcalophilus* phosphoserine aminotransferase. *Acta Crystallogr D*. 2013;69:804–811. doi:10.11 07/S0907444913002096
26. Yao J, Duan D, Song ZL, Zhang J, Fang J. Sanguinarine as a new chemical entity of thioredoxin reductase inhibitor to elicit oxidative stress and promote tumor cell apoptosis. *Free Radic Biol Med*. 2020. doi:10.1016/j.freeradbiomed.2020.01.008
27. Yu XA, Lu M, Luo Y, et al. A cancer-specific activatable theranostic nanodrug for enhanced therapeutic efficacy via amplification of oxidative stress. *Theranostics*. 2020;10(1):371–383. doi:10.7150/thno.39412
28. Cramer SL, Saha A, Liu J, et al. Systemic depletion of L-cyst(e)ine with cyst(e)inase increases reactive oxygen species and suppresses tumor growth. *Nat Med*. 2017;23(1):120–127. doi:10.1038/nm.4232
29. Ali SS, Ahsan H, Zia MK, Siddiqui T, Khan FH. Understanding oxidants and antioxidants: classical team with new players. *J Food Biochem*. 2020;44:e13145.
30. Ambrosone CB, Zirpoli GR, Hutson AD, et al. Dietary supplement use during chemotherapy and survival outcomes of patients with breast cancer enrolled in a cooperative group clinical trial (SWOG S0221). *J Clin Oncol*. 2019;JCO1901203.